Fermilab

A CERENKOV COUNTER DESIGN FOR A HIGH ENERGY,
HIGH INTENSITY SECONDARY BEAM

F. O. Borcherding

April 1986

A Cerenkov Counter Design

for a High Energy, High Intensity

Secondary Beam

by

Fred O. Borcherding

Facilities Support Department

Abstract

A cerenkov counter design is given for operation in a 500 GeV/c secondary beam with 10^9 to 10^{11} particles per 1 millisecond spill.

The design allows the fractions of pions, kaons and protons to be determined. In particular the fraction of kaons should be measured with a relative accuracy of a few percent.

Introduction

This paper reports on a design study for a cerenkov counter for use in the anticipated dichromatic neutrino beam[1], running at the higher Tevatron energies. The goal was to design a cerenkov counter which could measure the fractions of pions, kaons and protons to a few percent uncertainty. The previously built dichromatic train with a 500 GeV/c momentum setting and the already existing beamline layout was used as the operating environment.

In an effort to utilize the existing cerenkov counter mirror the concept of a compensating bend was developed which uses the astigmatic effect of an off axis mirror to compensate for the non-perfect optics of the dichromatic beam.

This report is divided into two major sections, a discussion of the expected beam and its properties and a discussion of the cerenkov counter and what determines its physical properties. Also included is a brief description of the counter layout in NC2.

I.A. Beam

The beam monte carlo programs used an input ray file generated by a modified Turtle[2] program using the Atherton[3] model for particle generation. Each output ray also had position information at two points interior to the train. This position information at the angle and momentum defining slit locations allowed one turtle file to be used for any slit setting desired by the cerenkov monte carlos.

Four sets of Turtle files were created called the TR, TF, TG and TX series. The TR files were for an early version of the train and are included here only for completeness. The TF files reflect the as built train which has an additional quadrupole, NC1Q6, added at the end of the train. The TG files were obtained by reoptimizing the magnet currents of the TF files with a new Transport run. The new optimization changed slightly the currents in NC1Q4 and NC1Q5 and changed the rotation and current in NC1UE. The last files TX are exactly the same as the TG files but with NC1Q6 turned off to study its effect.

I.B. CPHI Runs

A parabolic mirror will focus light from a point source onto a point image according to the equation

$$\frac{1}{S} \quad + \quad \frac{1}{S'} \quad = \quad \frac{1}{f} \qquad\qquad I.B.1$$

where S is the distance from the mirror to the source, S' is the distance from the mirror to the image and f is the focal length.

Consider the case where the particle rays all originate from a point source. If the particles were to emit cerenkov light at ϕ^0 relative to their direction then that light would focus to a point image at S'. If, however, the cerenkov light were emitted at some small angle, θ_c, the light would focus onto a ring on an image plane at S'. The radius of the ring would be

$$\rho = f \tan \theta_c. \qquad \text{I.B.2}$$

When the object has a finite size (m) the image also has a finite size (m') by the ratio

$$\frac{m'}{S'} = \frac{m}{S} \qquad \text{I.B.3}$$

The cerenkov ring will have a corresponding thickness given by

$$\Delta\rho = m' = m \frac{S'}{S} \qquad \text{I.B.4}$$

From this equation we see that the rings will have a root mean square (r.m.s.) thickness proportional to the r.m.s. beam spot size at the apparent source.

The position of the apparent source of the secondary beam was found as follows,

$$\Phi_x = \frac{\sigma_x \, rms}{Z} \quad .$$

The quantities Φ_x and Φ_y were defined as the beam spot size in x/y at distance Z upstream of the counter divided by Z. (See Reference 4 for a more detailed description). Φ is the root mean square of the sum of Φ_x and Φ_y. As the value of Z is increased Φ_x will in general decrease to a minimum value and then increase. A zero value of Φ_x at the minimum would indicate a point source in X. The program found foci in the horizontal(x) and vertical(y) directions both combined and separated. Figure I.B.1 shows a plot of Φ_x versus the distance upstream of NC2, the proposed location for the counter for the TG files. The minimum of Φ_x occurs 350m upstream. Figure I.B.2a shows the value of Φ_y which has a minimum at 1100m. Figure I.B.2b shows ϕ_y for Turtle file, TX, quad NC1Q6 off, and in this case the Z of the minimum is greater than 5000m. This effect illustrates the purpose for adding NC1Q6 which moves the point source in the vertical plane in from infinity.

The beam has two properties that limit the cerenkov counter resolution. The first is the finite size of the apparent source and is discussed further below. The second is that the minima of Φ_x and Φ_y occur at widely separated values of z. That is the beam appears to come not from a single point source but from two separate line sources, a property shared by most quadrupole focussed beams. It is not obvious how a simple optical system can simultaneously focus both sources.

I. B. 1   Φx versus Z.

The horizontal axis is the distance (in meters) upstream of the expansion port (NC2). The vertical axis is the r.m.s. beam spot size at Z in the horizontal plane divided by Z. This example is for pions of 500 GeV/c from the TG series of ray files with the LS series cuts at the collimators. The minimum or apparent source is 350m upstream.

PION   AT 327. METERS FROM TARGET

PHI X (MRAD) VS Z (M)
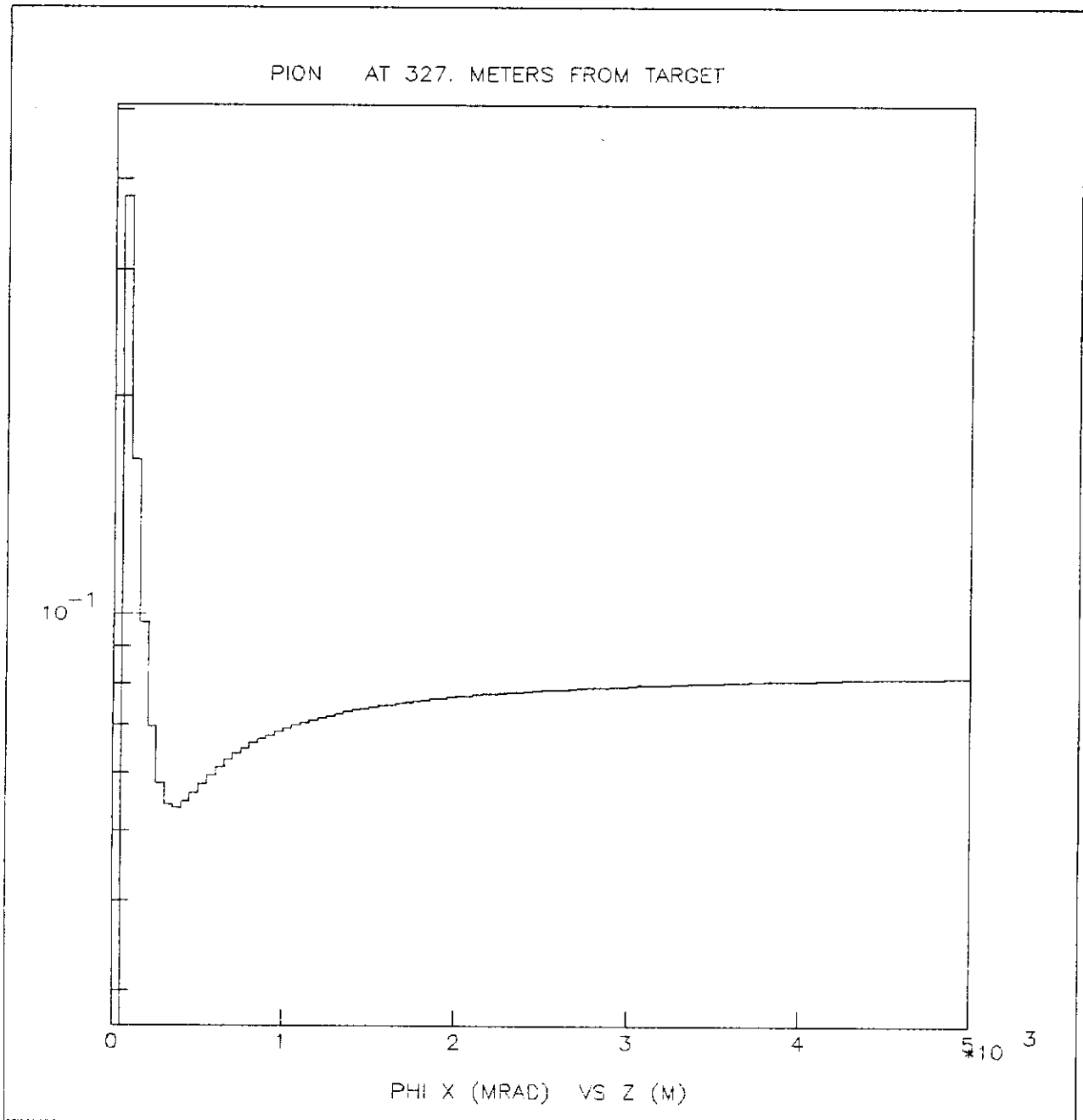
I. B. 2a   ⌀y   versus Z.

The horizontal axis is the distance (in meters) upstream of the expansion port (NC2). The vertical axis is the r.m.s. beam spot size at Z in the vertical plane divided by Z. The conditions are the same as for figure I.B.1. The minimum or apparent y source is 1100m upstream.

PION   AT 327. METERS FROM TARGET

PHI Y (MRAD) VS Z (M)
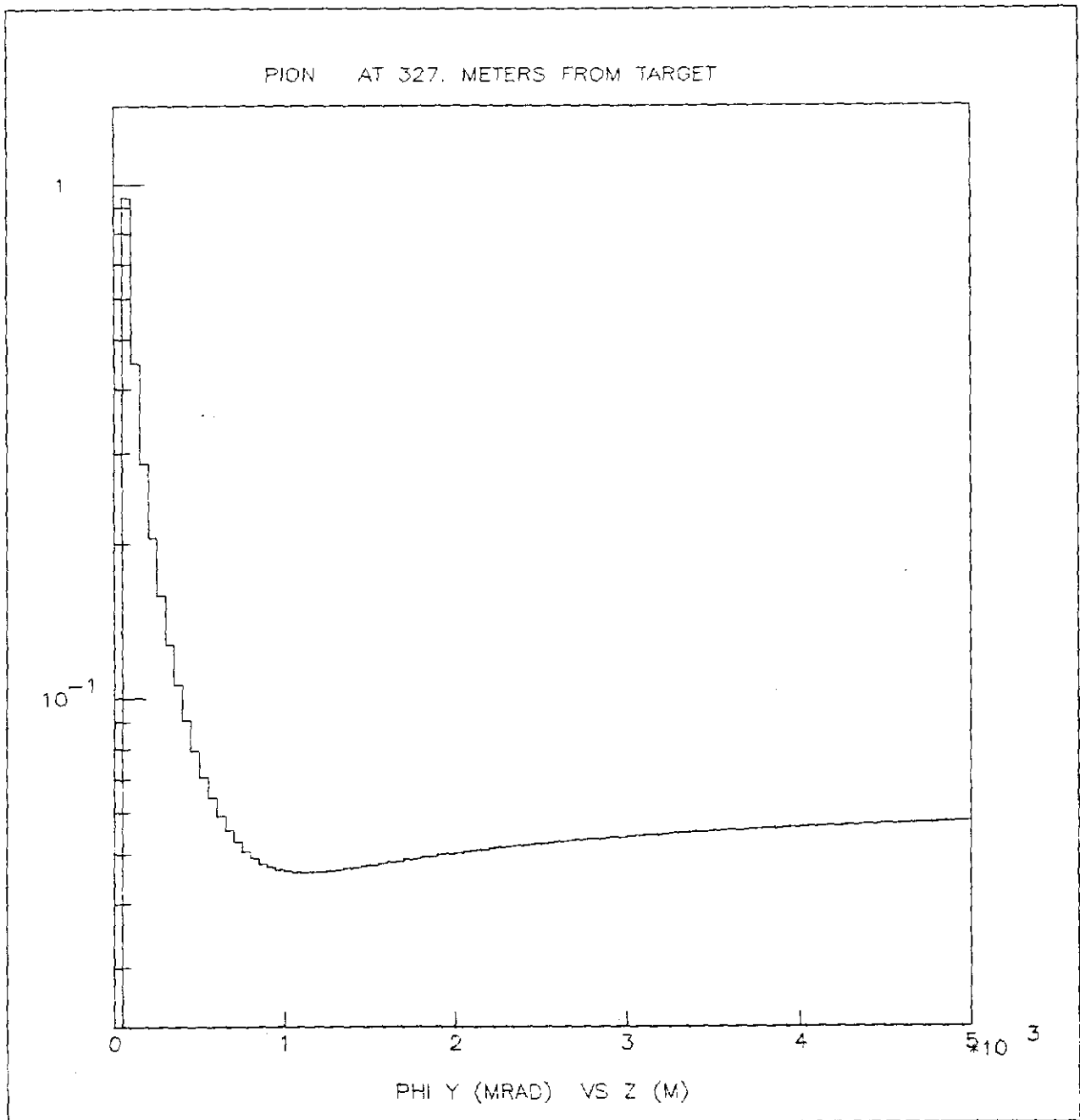
I. B. 2b ϕy   versus Z.

*The axis and conditions are the same as figure I.B.2a
except the input ray file is the TX series where the
final quadrupole is turned off. For this case there is
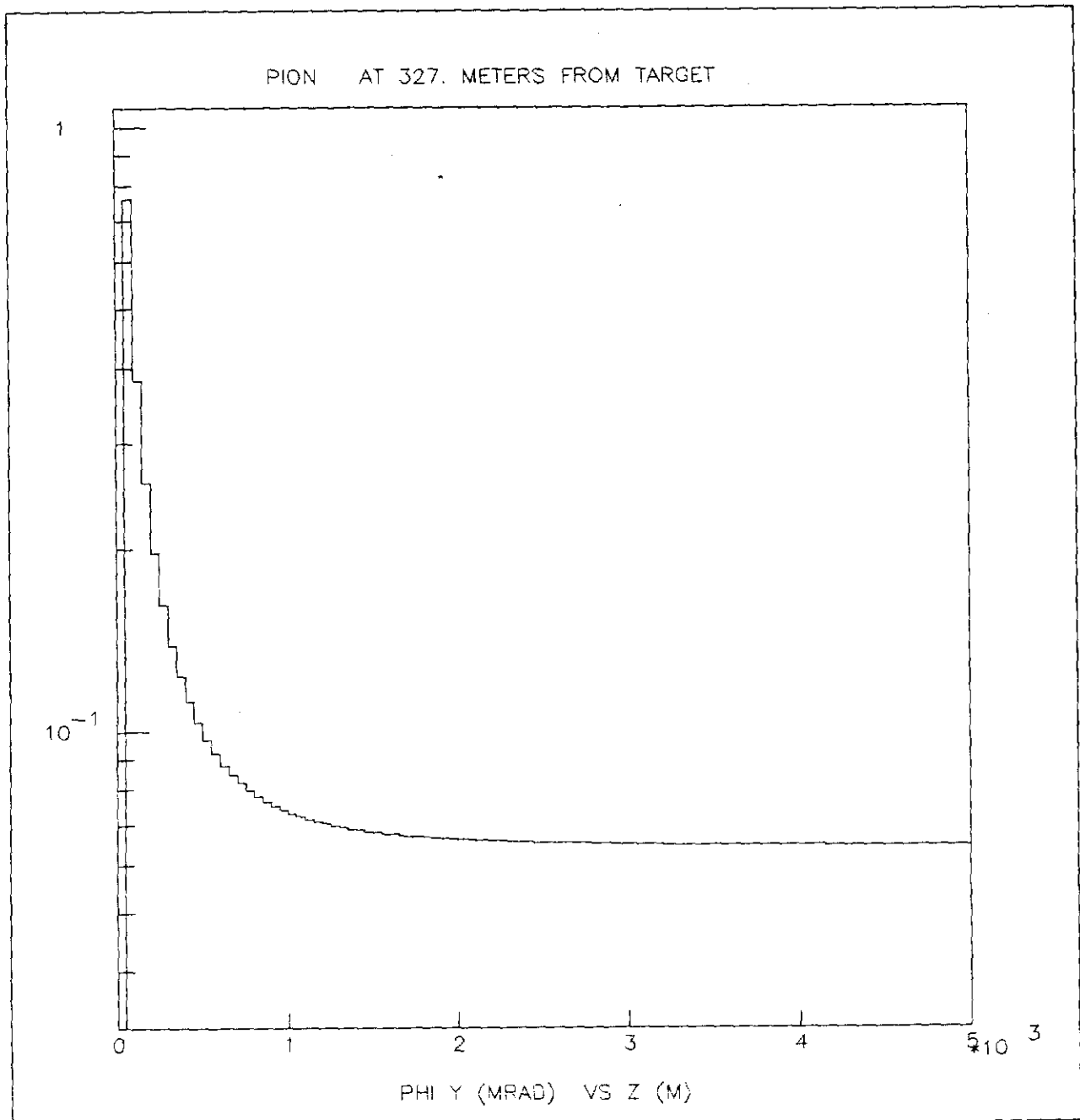no minimum or apparent focus.*

PION   AT 327. METERS FROM TARGET

PHI Y (MRAD) VS Z (M)

Table I.B.1 gives the values for Φ_x, Φ_y and Φ for the pion, kaon and proton ray files for the various cuts and Turtle input decks. The LS series cuts are the design angle and momentum cuts for the dichromatic[1]. The old cuts are tighter at the momentum slit and result in less angular dispersion as well as a higher mean beam momentum and less flux. Table I.B.2 gives the angular divergence and momentum values of the different ray files for different cuts. Table I.B.3. gives the beam spot size at NC2(and for completeness NC3).

II. Cerenkov Counter

There are many effects which broaden the cerenkov ring. Effects that were studied included the length of the cerenkov radiator, the momentum dispersion of the beam, the difference of the beam from a point source and astigmatism due to an off axis mirror. This section will discuss these four effects and show how to combine the last two with a compensating bend of the cerenkov mirror to improve the cerenkov counter performance.

II.A. Counter Length

The diffraction broadening effect of a finite length (L) counter is discussed in detail in Reference 5. Equation 10 of that reference is

$$x(\theta) = \pi \left(\frac{L}{\lambda}\right) \left(\frac{1}{n\beta} - \cos\theta \right) \qquad \text{II.A.1}$$

where the light intensity is proportional to

$$\left(\frac{\sin x}{x}\right)^2 \quad . \qquad \text{II.A.2}$$

TABLE I. B. 1

APPARENT BEAM SOURCE POSITION

IN METERS UPSTREAM OF THE ENCLOSURE

FOR THE EXPANSION PORT (NC2) AND THE MANHOLE (NC3)

File	z of minimum in horizontal (x) plane			z of minimum in vertical (y) plane			z of minimum in combined x/y planes		
	pion	kaon	proton	pion	kaon	proton	pion	kaon	proton
NC2									
LS cuts									
TG	350	350	425	1100	1025	825	800	750	700
TF	350	350	400	1125	1025	825	800	775	700
TR	350	350	400	5000+	5000+	1900	1325	1100	950
TX	350	350	400	5000+	5000+	1750	1200	1075	925
Old cuts									
TG	350	350	450	975	925	800	700	750	700
TF	350	350	425	1100	925	800	750	750	700
TR	350	350	350	5000+	3100	1600	1200	1100	950
TX	375	350	400	5000+	2925	1550	1150	1000	900
NC3									
LS cuts									
TG	450	450	500	1225	1175	1000	825	800	825
TF	400	450	500	1250	1175	1100	800	800	800
TR	450	450	500	3100	2150	1575	875	850	900
TX	450	500	550	2250	1750	1475	875	850	900
Old cuts									
TG	450	450	550	1175	1100	950	800	825	850
TF	425	450	550	1175	1125	975	800	825	825
TX	475	500	550	2525	1950	1475	925	925	925

This table gives the results of the CPHI program on the TG turtle files for two sets of cuts. The number given is the distance, z, in meters upstream of the counter position of the minimum of the χ value.

TABLE I. B. 2.

BEAM DIVERGENCE AND MOMENTUM

	(θx)			(θy)			P +- dP (GeV) (r.m.s.)		
	pion	kaon	proton	pion	kaon	proton	pion	kaon	proton
LS cuts									
TG	.074	.080	.070	.064	.072	.080	490 +-44	492 +-48	511 +-50
TF	.076	.081	.071	.064	.072	.081	490 +-44	492 +-48	511 +-50
TR	.077	.084	.075	.058	.064	.060	491 +-40	493 +-44	509 +-46
TX	.073	.080	.074	.064	.071	.064	490 +-44	493 +-49	511 +-50
Old cuts									
TG	.058	.066	.060	.066	.074	.083	500 +-41	503 +-46	519 +-47
TF	.059	.066	.060	.066	.073	.083	500 +-41	502 +-45	519 +-47
TR	.063	.071	.066	.049	.054	.056	502 +-37	505 +-41	519 +-43
TX	.064	.072	.069	.056	.062	.060	500 +-41	503 +-46	519 +-47

In the first six columns the tabulated quantity is the r.m.s. in mrad of the distribution of the angles of the Turtle rays passing the given cuts. In the last three columns the tabulated quantity is the mean beam momentum followed by the r.m.s. momentum spread.

TABLE I. B. 3

BEAM SPOT SIZE AT THE ENCLOSURES IN CM

	Expansion Port NC2						Manhole NC3					
	x spot (r.m.s.)			y spot (r.m.s.)			x spot (r.m.s.)			y spot (r.m.s.)		
file	pion	kaon	proton	pion	kaon	proton	pion	kaon	proton	pion	kaon	proton
LS cuts												
TG	2.08	2.34	2.38	4.91	5.14	5.54	2.85	3.12	3.08	5.31	5.52	5.94
TF	2.12	2.33	2.40	4.88	5.09	5.52	2.88	3.14	3.12	5.25	5.48	5.94
TR	2.24	2.46	2.50	3.79	4.00	4.42	3.11	3.34	3.38	3.86	4.16	4.71
TX	2.33	2.59	2.70	3.80	4.02	4.46	3.09	3.36	3.50	3.90	4.20	4.72
Old cuts												
TG	2.12	2.35	2.39	5.19	5.42	5.72	2.74	3.02	3.04	5.67	5.86	6.17
TF	2.12	2.33	2.42	5.16	5.38	5.72	2.73	3.00	3.08	5.60	5.82	6.19
TR	2.27	2.44	2.50	4.10	4.32	4.65						
TX	2.41	2.65	2.72	4.07	4.29	4.64						

The tabulated quantity is the r.m.s. beam spot size in cm at the given enclosure for the pion, kaon and proton components of the beam individually.

Solving equation II.A.1 for $\cos\theta$ gives

$$\cos\theta = \frac{1}{n\beta} - \frac{x\lambda}{\pi L} \qquad\qquad \text{II.A.3}$$

The principle cerenkov angle is at $x=\emptyset$ and

$$\cos\theta_c = \frac{1}{n\beta} \qquad\qquad \text{II.A.4}$$

the familiar equation for the cerenkov angle. At the first diffraction minimum $x = \pi$ and

$$\cos (\theta_c + \Delta\theta) = \frac{1}{n\beta} - \frac{\lambda}{L} \qquad\qquad \text{II.A.5}$$

so

and

$$-\sin\theta\Delta\theta = \cos (\theta_c + \Delta\theta) - \cos\theta_c = \frac{-\lambda}{L} \qquad\qquad \text{II.A.6}$$

and

$$\Delta\theta = \frac{-\lambda}{L\theta_c} \qquad\qquad \text{II.A.7}$$

for small θ_c.

From equation I.B.2

$$\Delta\rho = f\Delta\theta \qquad\qquad \text{II.A.8}$$

and combining with equation II.A.7 gives

$$\Delta\rho = \frac{f\lambda}{L\theta_c} \qquad . \qquad\qquad \text{II.A.9}$$

At 12Hgmm of helium gas for pions at 500 GeV/c we have $\theta_c = 0.975$ mrad, $f = 302.26$cm and $\lambda = 0.6\mu$m.

$$\Delta\rho \text{ (cm)} = (0.186) / L(m) \qquad\qquad \text{II.A.10}$$

and

$$\frac{\Delta\rho}{\rho} = \frac{\lambda}{L\theta_c{}^2} = (0.631) / L(m) \qquad\qquad \text{II .A.11}$$

Table II.A.1 shows the values of Δp and $\Delta p/p$ for several values of L. For 2m, the length of the old counter the calculated $\Delta p/p$ is about 30%. If the counter is increased to 50m then the calculated $\Delta p/p$ drops to 1%.

The fourth column of the table gives the Δp for the standard monte carlo output with only the radiator length varied. For short counters the diffraction effect can be seen to dominate the peak width while for counters longer than 10m other effects dominate.

Figure II.A.1 shows a plot of relative light intensity from pions at 12 Hgmm of helium gas versus the radius of the cerenkov ray's intersection with the detector for a 50 meter counter. For Figure II.A.2 all the conditions are the same but now the counter is only 2m long. For the 2m counter the peak has broadened considerably and the large radius tail has increased dramatically. This tail is from light emitted at angles greater than θ_c. Clearly a 2m radiator length is not suitable for particle separation.
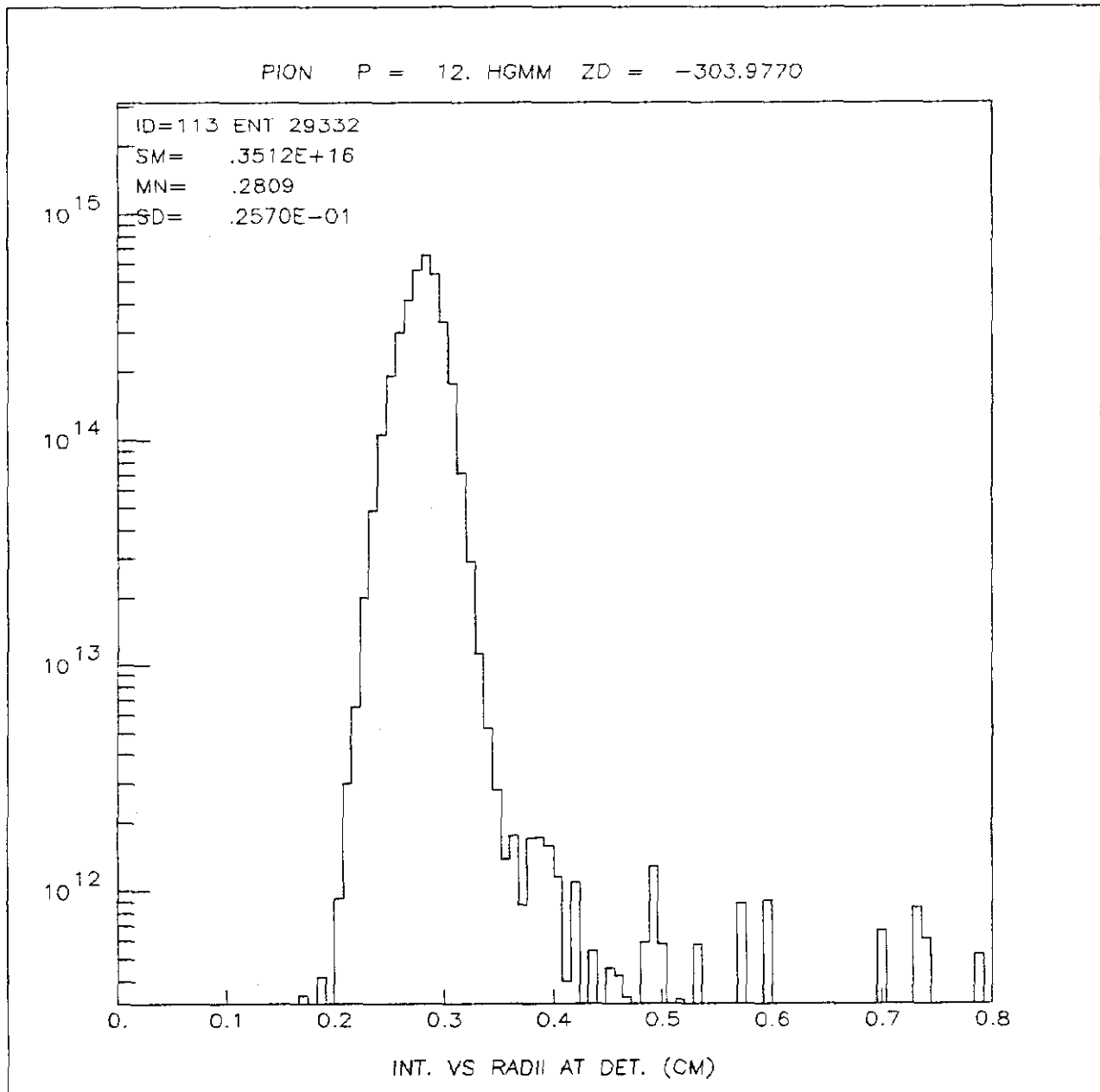
TABLE II. A. 1.

CERENKOV RING WIDTH FOR 0 = 1 mrad

length (m)	Calculated		Monte Carlo	
	$\Delta\rho$ (cm)	$\Delta\rho/\rho$	$\Delta\rho$ (cm)	$\Delta\rho/\rho$
1	.186	.63	.111	.32
2	.093	.32	.084	.26
5	.037	.13	.058	.19
10	.0186	.06	.042	.14
20	.0093	.03	.032	.11
50	.0037	.01	.025	.09
70	.0027	.01	.025	.09

This table gives for various counter lengths the width of the cerenkov ring. The calculated columns are using the equations derived in the text. The monte carlo columns are the r.m.s. peak width of intensity versus radius distributions. The input beam was the standard TG ray file with the standard cuts.
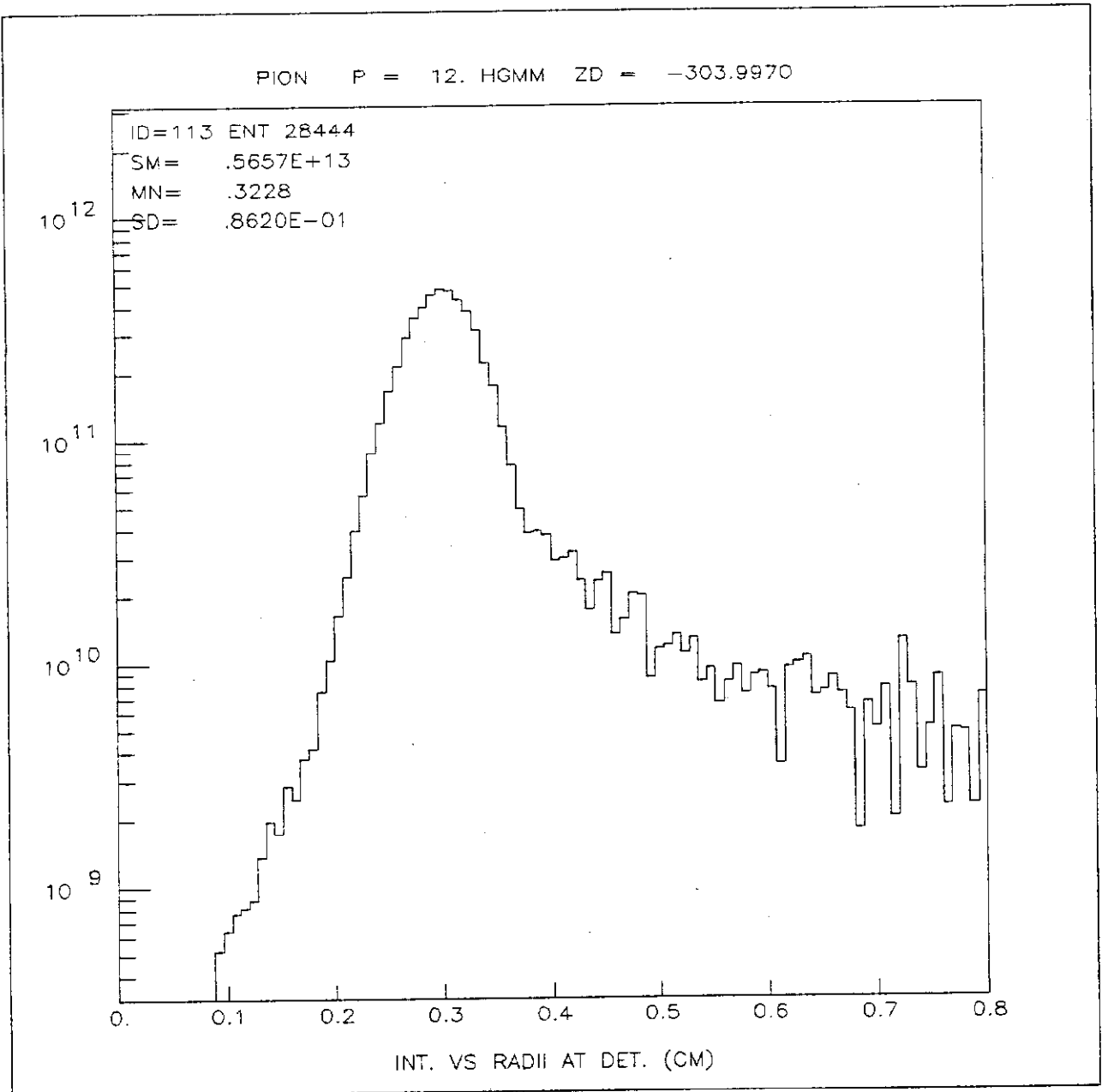
II. A. 1 Pion Peak Standard Configuration
at 12Hgmm.

The vertical axis is the relative cerenkov light
intensity in number of photons per 0.008cm radial bin
as seen by a CCD with a typical spectral sensitivity.
The horizontal axis is the radial distance from the
center of the cerenkov ring. The plane of the detector
is at 303.977cm from the mirror and the gas pressure is
12Hgmm. For the standard configuration the length of
radiator is 50m and the mirror is rotated off axis by
4.37 degrees in the horizontal plane. Also the TG
series of ray files are used with the LS series
collimator cuts.

PION   P =   12. HGMM ZD =   −303.9770

ID=113 ENT 29332
SM=   .3512E+16
MN=   .2809
SD=   .2570E−01

INT. VS RADII AT DET. (CM)

II. A. 2   Pion Peak for a 2m Radiator

The axis and conditions are the same as for figure II.A.1 except the length of the radiator has been reduced to 2m. Diffraction effects now dominate as evidenced by the broadened peak and the large radius tail.

PION   P = 12. HGMM   ZD = −303.9970

ID=113 ENT 28444
SM=   .5657E+13
MN=   .3228
SD=   .8620E−01

INT. VS RADII AT DET. (CM)

II.B.   Beam Source Size

The peak width for the pions in Figure II.A.1 is dominated by the spot size m of the beam at the source S. Using equation I.B.2 for ρ and I.B.4 for Δp we get

$$\frac{\Delta \rho}{\rho} \quad = \quad \frac{S'}{f} \quad \cdot \quad \frac{m}{S \tan \theta_c} \qquad\qquad \text{II.B.1}$$

The σ_x r.m.s of equation I.B.5 is the source size m so we can substitute and get

$$\frac{\Delta \rho}{\rho} \quad = \quad \frac{S'}{f} \quad \cdot \quad \frac{\phi}{\theta_c} \qquad\qquad \text{II.B.2}$$

for θ_c small.

For pions at 500 GeV and LS cuts

$$\phi_x = 0.538 \times 10^{-4} \text{ rad}$$

and at 12 Hgmm

$$\theta_c = .87 \times 10^{-3} \text{ rad}$$

$$S' = 304.0 \text{ cm}$$

$$f = 302.3 \text{ cm}$$

so

$$-\frac{\Delta\rho}{\rho} \quad = 6.2 \times 10^{-2} \qquad\qquad\qquad\qquad \text{II.B.3}$$

and ρ = .28 cm from the figure so

$$\Delta\rho = .17 \times 10^{-1} \text{ cm}$$

which accounts for 90% of the peak width.

II.C. Momentum Dispersion

The familiar equation for cerenkov radiation is

$$\cos\theta_c \quad = \quad \frac{1}{\beta n} \qquad\qquad\qquad\qquad \text{II.C.1}$$

Using this to find the variation of θ_c with momentum we have substituting for β,

$$\cos\theta_c \quad = \quad \left(\frac{1}{n} \right) \left(1 + \frac{m^2}{p^2} \right)^{+} \qquad\qquad \text{II.C.2}$$

Taking the derivative with respect to p gives,

$$\sin\theta_c \Delta\theta_c = \left(\frac{1}{n}\right)\left(1 + \frac{m^2}{p^2}\right)^{-} \quad \left(\frac{m^2 \Delta p}{p^3}\right) \quad . \qquad \text{II.C.3}$$

Assuming a small angle and m/p << 1 gives

$$\Delta\theta c = \left(\frac{1}{n\theta_c} \right) \cdot \left(\frac{\Delta p}{p} \right) \cdot \frac{m^2}{p^2}$$ II.C.4

And substituting equation II.A.2 for $\Delta\theta_c$

$$\Delta\rho = \left(\frac{f}{n\theta_c} \right) \left(-\frac{\Delta p}{p} \right) \left(-\frac{m^2}{p^2} \right)$$ II.C.5

Table II.C.1 gives the momentum dispersion contribution to the cerenkov peak width for pions and kaons at 12Hgmm with a 500 GeV/c beam. The contribution to the pion peak width is small, but for the kaon peak this is the major contribution.

Figure II.C.1 shows the relative intensity versus radius for cerenkov light from kaons for the standard counter at 22Hgmm. The contribution to the peak width from the 10% momentum bite is, from equation II.B.5.

$$D\rho = (.10) \left(\frac{302.3cm}{.92 \times 10^{-3} rad} \right) \left(-\frac{.494}{500} \right)$$
$$\Delta\rho = .032cm$$ II.C.6

Figure II.C.2 shows the same kaon peak with the momentum bite in the monte carlo set to zero.
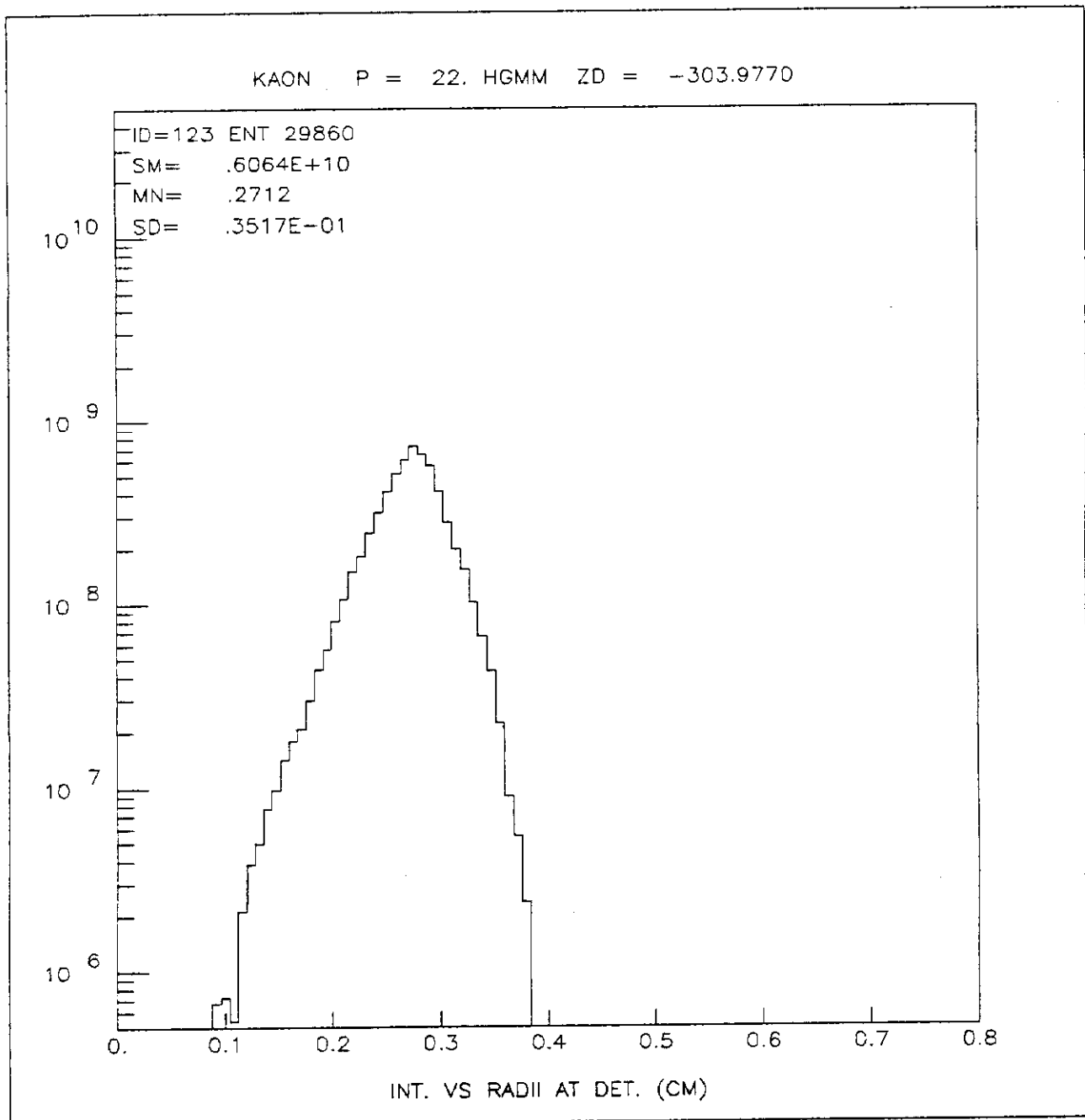
TABLE II. C. 1

MOMENTUM BITE CONTRIBUTION TO PEAK WIDTH

Momentum Bite in %	pion (cm)	kaon (cm)
1.	.00024	.0066
5.	.0012	.033
10.	.0024	.066
15.	.0036	.098

The tabulated values are the cerenkov ring r.m.s. widths in cm for pions and kaons calculated with equation II.C.5.
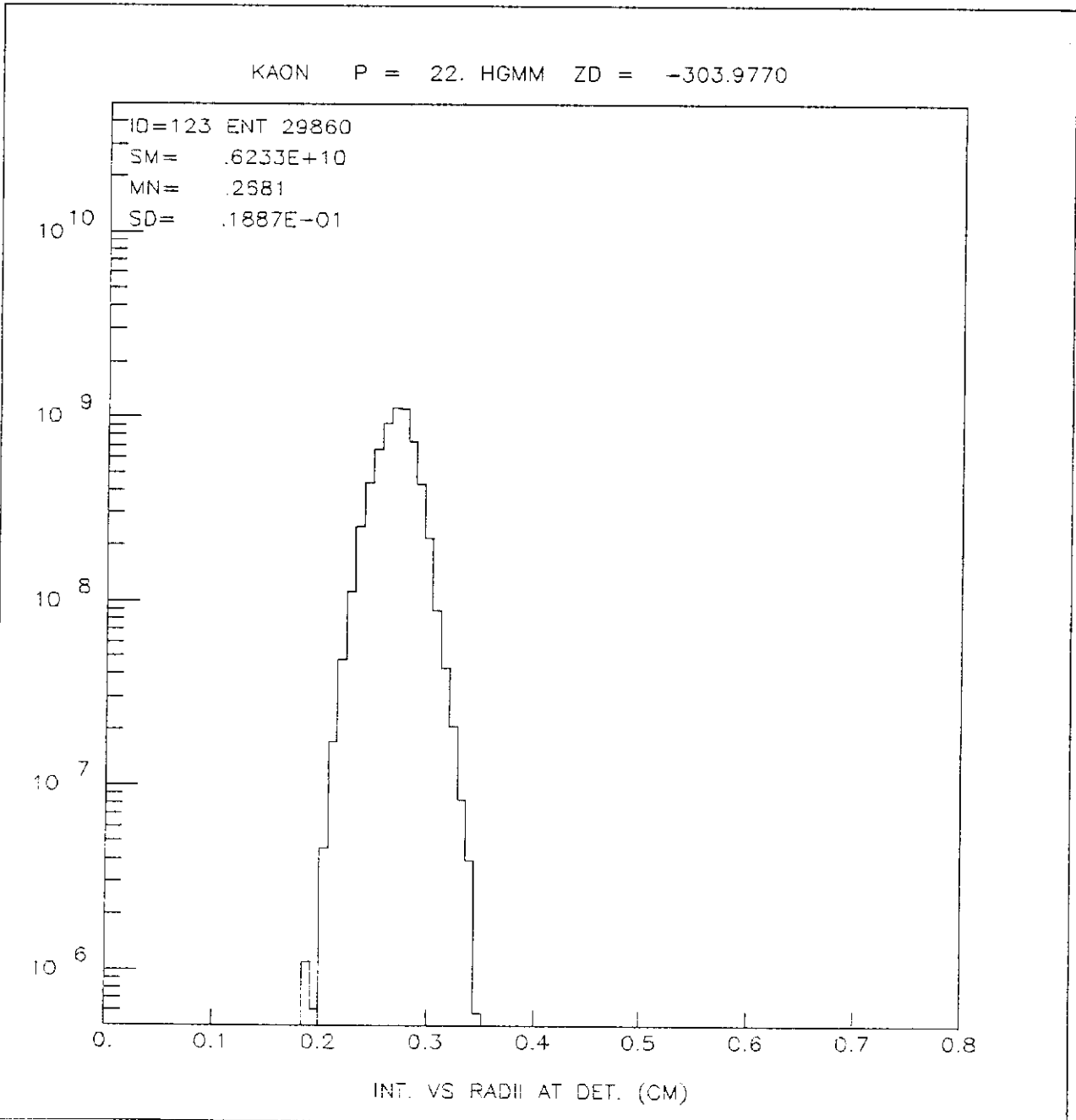
II. C. 1   Kaon Peak for Normal Momentum Bite

The vertical axis is the relative number of detected cerenkov photons per 0.008cm radial bin for a standard configuration at a gas pressure of 22Hgmm. The horizontal axis is the distance in cm from the center of the cerenkov ring.

KAON   P =   22. HGMM   ZD =   −303.9770

ID=123 ENT 29860
SM=   .6064E+10
MN=   .2712
SD=   .3517E−01

INT. VS RADII AT DET. (CM)

II. C. 2   Kaon Peak for a Monoenergetic Beam

The axis and conditions are the same as for figure
II.C.1 but the kaon momentum has been set to exactly
500 GeV/c for all rays. A comparison of C.1 to C.2
shows the effect of the momentum bite of the beam on
the width of the cerenkov peak of the kaon.

KAON   P =   22. HGMM   ZD =   -303.9770

ID=123 ENT 29860
SM=   .6233E+10
MN=   .2681
SD=   .1887E-01

INT. VS RADII AT DET. (CM)

If we add the peak width for figure II.C.2 in quadrature with the calculated contribution from the momentum bite we get

$$\Delta\rho = 0.37\text{cm},$$

which is in good agreement with the peak width of Figure II.C.1. The momentum dispersion contributes over 90% of the kaon peak width.

II.D Compensating Bend

For sources not on the mirror axis an image defect known as astigmatism occurs. Let a source be displaced from the axis in one plane called the tangential plane and be on the axis in the sagittal plane. Let α be the angle between a line from the source to the center of the mirror and a line along the mirror axis. Alternatively let α be the angle of rotation of the mirror in the tangential plane. Then[6]:

$$\frac{1}{S} + \frac{1}{S'_t} = \frac{1}{f\cos\alpha} \quad , \qquad \text{II.D.1a}$$

$$\frac{1}{S} + \frac{1}{S'_s} = \frac{\cos\alpha}{f} \quad ; \qquad \text{II.D.1b}$$

where S is the distance to the source, f is the focal length of the mirror, S'_t is the distance to the tangential focus and S'_s is the distance to the sagittal focus. From these equations we see that $S'_t < S'_s$ for $\alpha \neq 0°$. A point source will in fact focus onto two mutually perpendicular line images at S'_t and S'_s. The dichromatic beam, however,

seems to have different line sources in the x and y planes. Writing equations II.C.1 when the source point is different in each plane gives;

$$-\frac{1}{S_t} \quad + \quad -\frac{1}{S_t'} \quad = \quad \frac{1}{f\cos\alpha} \qquad\qquad \text{II.D.1}$$

$$-\frac{1}{S_s} \quad + \quad -\frac{1}{S_t'} \quad = \quad \frac{\cos\alpha}{f} \qquad\qquad \text{II.D.2}$$

By requiring $S_s' = S_t'$ and solving the equations for $\cos\alpha$ gives,

$$\cos\alpha = \frac{-k + k^2 + 4}{2} \qquad\qquad \text{II.D.3}$$

where

$$k = f \left(-\frac{1}{S_t} \quad - \quad -\frac{1}{S_s} \right) \qquad\qquad \text{II.D.4}$$

For the dichromatic beam k will be small so the positive root must be taken for $\cos\alpha$ to be close to one.

$$\cos\alpha = \frac{k^2 + 4 - k}{2} \qquad\qquad \text{II.D.5}$$

and k must be positive for $\cos\alpha \leq 1$, which leads to

$$S_s > S_t. \qquad\qquad \text{II.D.6}$$

To see the size of this effect we have used a monte carlo simulation of the cerenkov counter with a special input particle beam. In this monte carlo the beam spot size at the counter was given by a random gaussian distribution in x and y and the beam divergence was made to be,

$$\theta_x = x/S_x$$

and

<div align="right">II.D.7</div>

$$\theta_y = y/S_y,$$

where S_x and S_y are the distances to the x and y source points. For the dichromatic beam with L cuts the apparent sources are at 350m and 1100m. Therefore let

$$S_s = S_x = 1100m \qquad \text{II.D.8}$$

and

$$S_t = S_y = 350m.$$

For these two source positions

$$S'_x = 304.09cm$$

and

<div align="right">II.D.9</div>

$$S'_y = 304.89cm,$$

without any mirror rotation. Table II.D.1 gives the results of a monte carlo run for this case. The ZD column is the position of the detector plane which in five steps moves from the optimum for S_y to the optimum for S_x. The next two columns are the r.m.s. of the distribution of the x/y positions of cerenkov photons emitted at 0^0 (Restricting the light emission to 0^0 avoids complications from cerenkov emission and allows us to see the effects of the optics directly). The spot size varies greatly with the detector plane position. The smallest spot size of .007cm should be compared with .005cm, the r.m.s., value of $S_x=S_y=1100cm$ and $\alpha = 0^0$. At the plane of least confusion (304.993cm) the spot sizes are .015cm.

Next consider the case when

$$S_x = S_y = 1100cm; \qquad\qquad II.D.10$$

the mirror is rotated, $\alpha = 4.39^0$.

This case is also shown in Table II.D.1. Here the r.m.s. at the plane of least confusion is about .016cm. Also notice the x and y values are nearly reversed from the on axis case above.

Now consider the case of compensating bend,

$$S_x = 1100m,$$

$$S_y = 350m \qquad\qquad II.D.11$$

TABLE II. D. 1.

CERENKOV SPOT SIZE

ZD (cm)	sigma x (cm)	sigma y (cm)

Dual line source beam with an on axis mirror
  Sx = 1100m   Sy = 350m   rotation = 0 degrees

ZD (cm)	sigma x (cm)	sigma y (cm)
304.89	.023	.008
304.44	.019	.011
304.99	.015	.015
304.54	.011	.019
304.09	.007	.023

Point source beam with an off axis mirror
  Sx = 1100m   Sy = 1100m   rotation = 4.39 degrees

ZD (cm)	sigma x (cm)	sigma y (cm)
303.99	.008	.024
303.54	.011	.020
303.09	.015	.017
302.64	.019	.013
302.19	.023	.010

Dual line source beam with a compensating bend
  Sx = 1100m   Sy = 350m   rotation = 4.39 degrees

ZD (cm)	sigma x (cm)	sigma y (cm)
304.49	.009	.012
304.24	.006	.009
303.99	.005	.007
303.74	.006	.009
303.49	.009	.012

    This table gives the spot size for cerenkov light emitted at
zero degrees with the detector plane at various positions for
three types of beam. For the dual line source beam the particles
came from two line sources at the positions given.

and from equation II.D.5

$$\alpha = 4.39^0.$$

Table II.D.1 shows a spot size of .008cm at the compensating focal plane of 303.99cm. For these three cases the compensating bend gives the best simultaneous focus in x and y. Indeed it is even better than the best x and y spots.

Figures II.D.1a and 1b show pressure plots for the standard Turtle beam for mirror rotations of 0^0 and 4.34^0. For these plots the horizontal axis is the gas pressure in Hgmm and the vertical axis is the relative light intensity passing through a circular iris subtending an angle of + 0.3 mrad. The pressure curve with an iris technique was used to gather data using previous cerenkov counters. Figure II.D.1a is for the compensating bend case and Figure II.D.1b is for an on axis mirror. The low pressure edges of each peak are the same on both plots. The high pressure edges, however, have been lowered significantly in the compensating bend case. Here the compensating bend is clearly superior to an on axis mirror. Figures II.D.2a and 2b show the same Turtle beam with the cerenkov data plotted as intensity versus radius on the detector plane. For the light from pions at 6Hgmm the inner edge of the ring has moved well out of zero. The compensating bend case Fig. 2a with peak sigma of .017 cm is 85% of the width of the on axis case Fig. 2b while the means are the same. Here again the compensating bend case is superior to an on axis mirror.

II. D. 1a   Intensity versus Pressure
for a Compensating Bend

The vertical axis is the relative number of cerenkov photons seen by the detector inside a circle subtending .3mrad at the detector plane. The horizontal axis is the helium gas pressure in Hgmm. For the compensating bend the off axis angle of the mirror and the position of the detector plane is calculated from the position of the apparent sources in the horizontal and vertical projections of the beam. For this case the horizontal source is 350m upstream and the vertical 1100m. The off axis angle is therefore 4.37 degrees and the focal plane at 303.977cm.
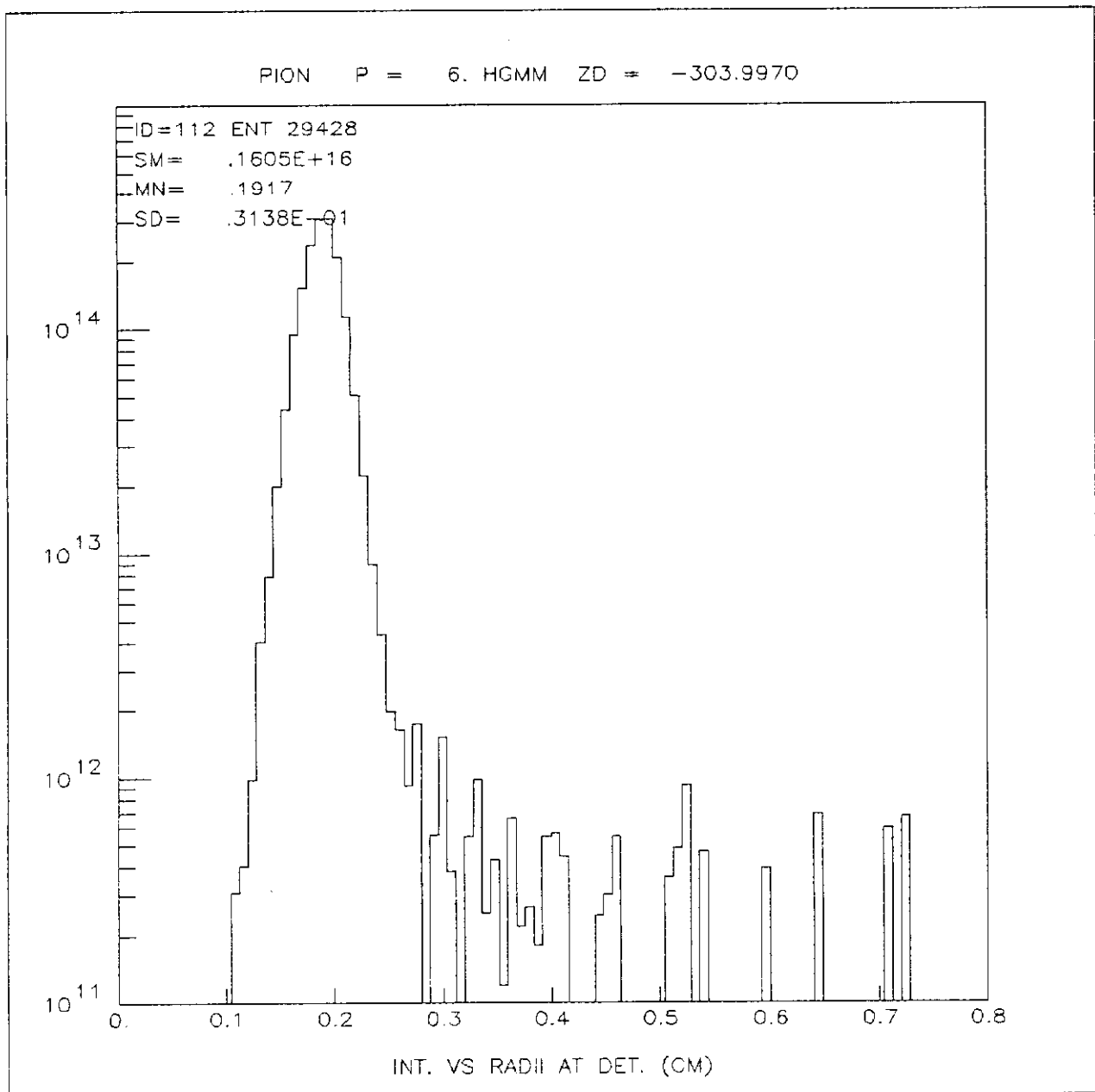
COMBINED PLOT FOR   500. GEV FROM   .00 TO   60.00 MMHG

INT VS PRES. ZIR= -303.977
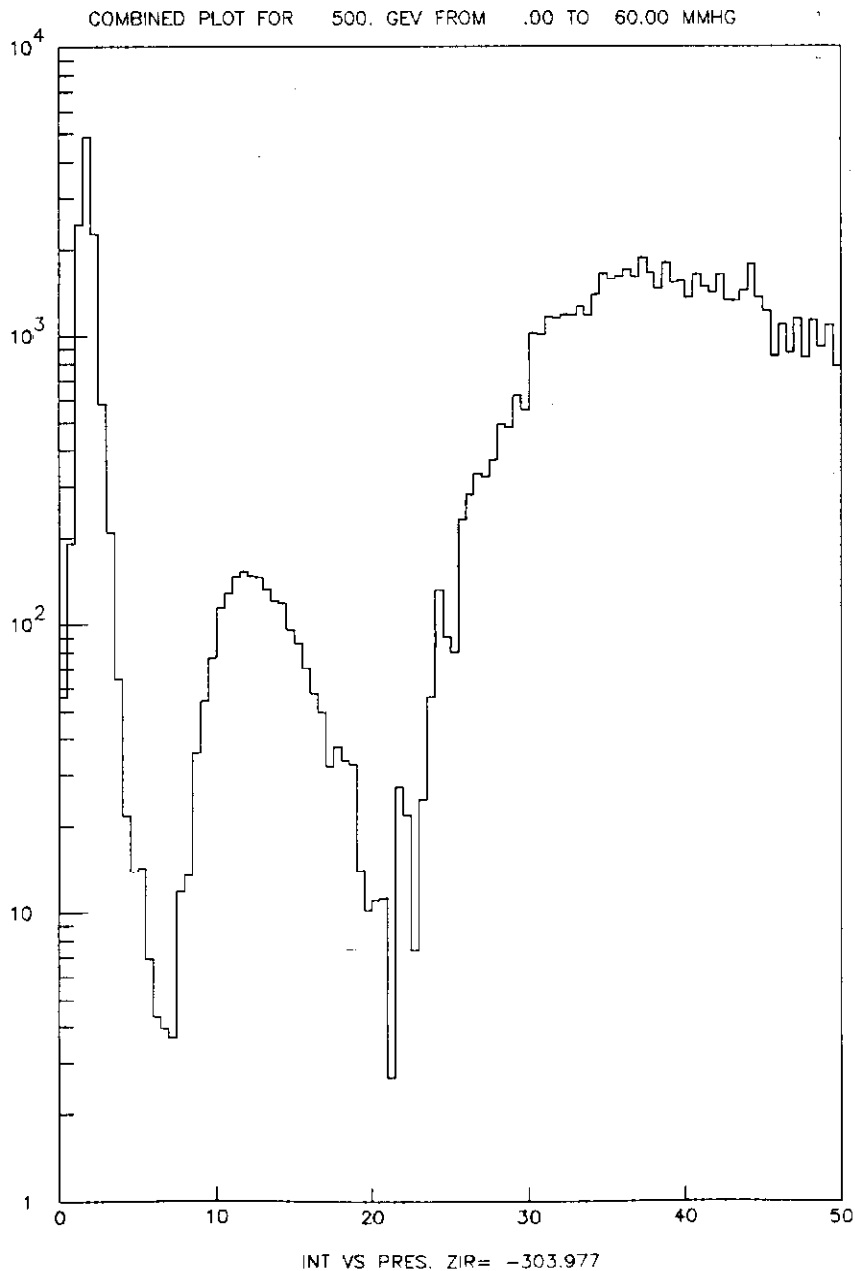
II. D. 1b   Intensity versus Pressure for an
On Axis Mirror

The axes and conditions are the same as figure II.D.1a except the mirror is not rotated and the dector plane is the plane of least confusion. Comparison of this figure to 1a shows that using a compensating bend is better than an on axis mirror for this beam with separated apparent images.
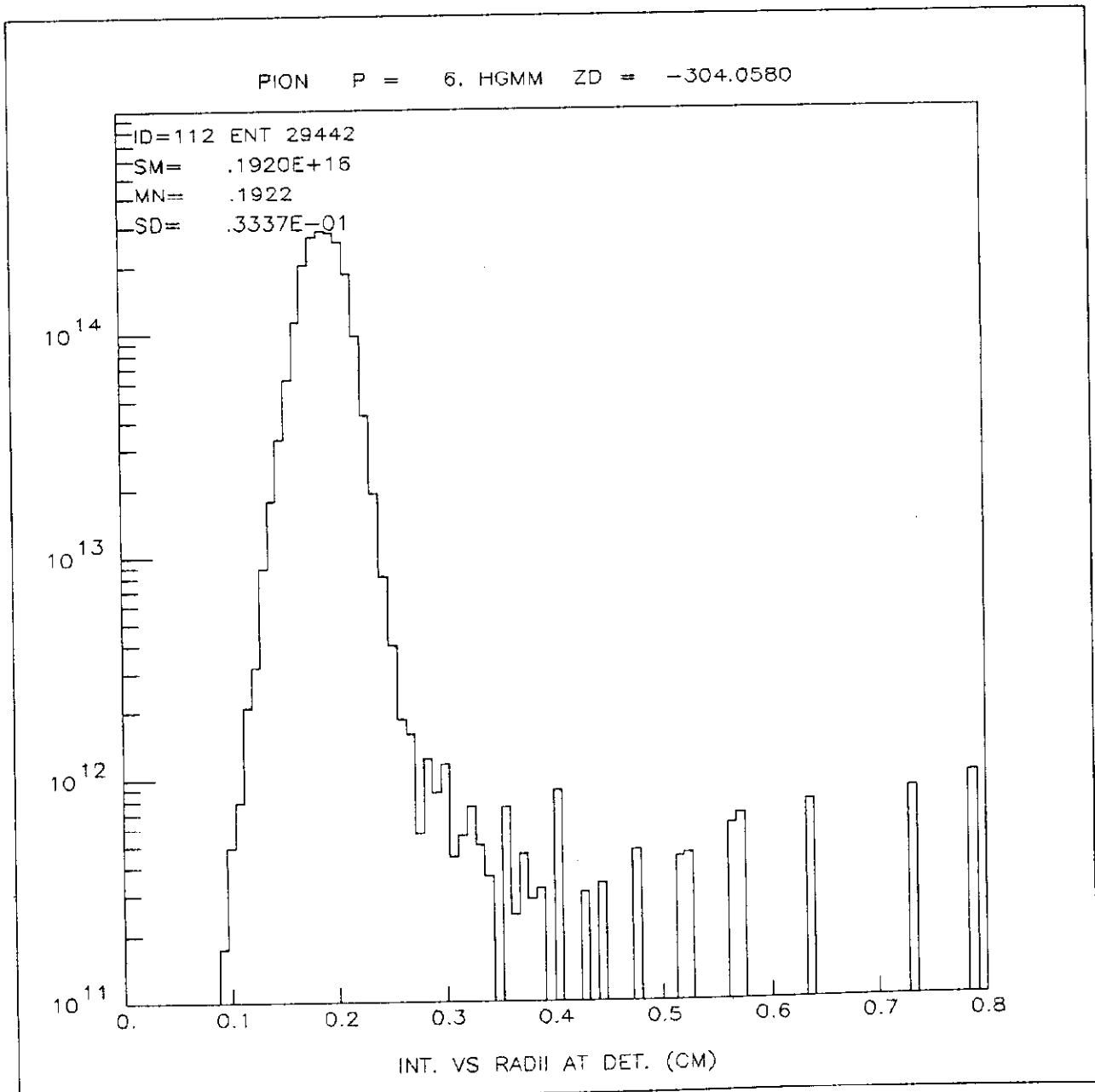
COMBINED PLOT FOR   500. GEV FROM   .00 TO   60.00 MMHG

INT VS PRES. ZIR= −304.058
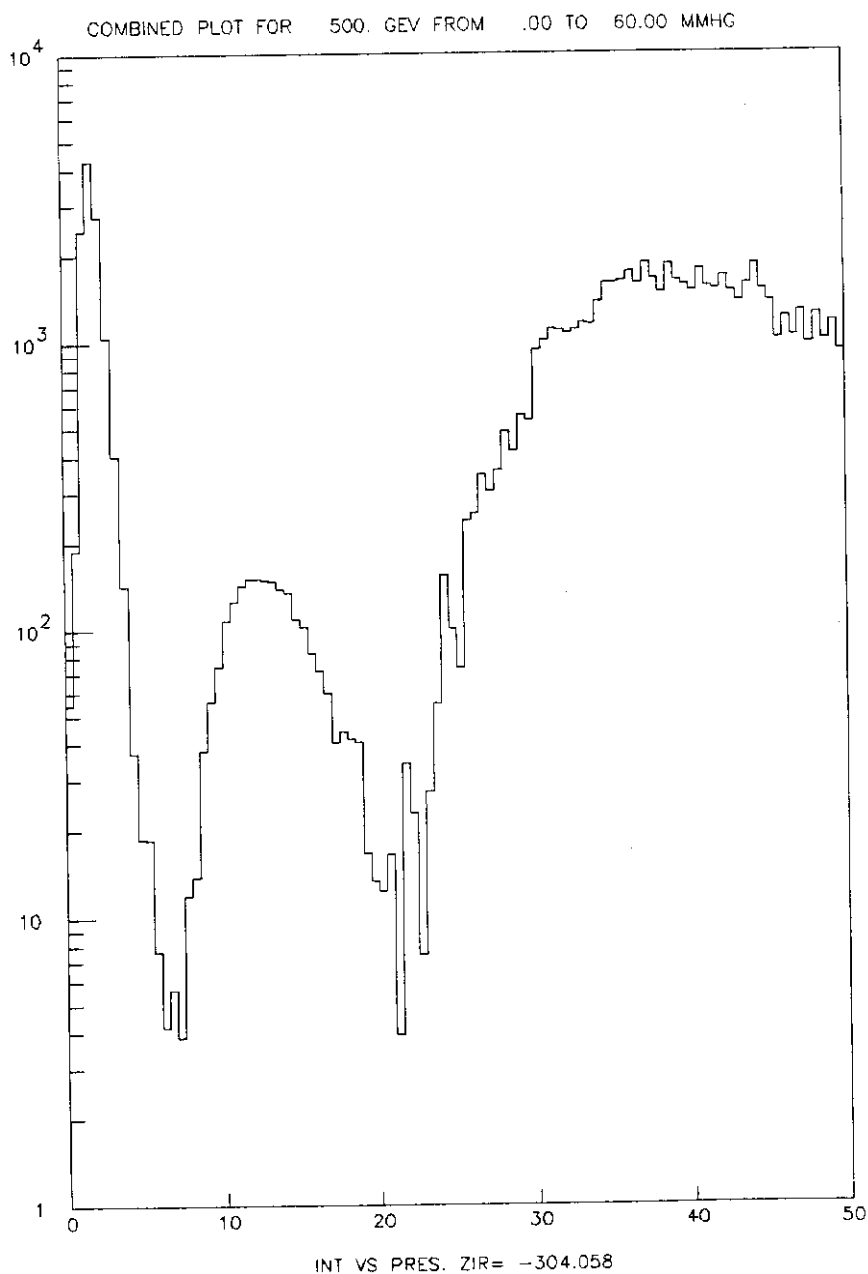
II. D. 2a   Pion Peak for the Standard Configuration
at 6Hgmm

The vertical axis is the relative number of cerenkov
photons per 0.008cm radial bin. The horizontal axis is
the distance in cm from the center of the cerenkov
ring. This is for the standard configuration which has
a compensating bend of 4.37 degrees and uses a 50m long
radiator.

PION   P =   6. HGMM   ZD =   −303.9970

ID=112 ENT 29428
SM=   .1605E+16
MN=   .1917
SD=   .3138E−01

INT. VS RADII AT DET. (CM)

II. D. 2b   Pion Peak for an On Axis Mirror

The axis and conditions are the same as figure 2a
except the mirror is not rotated and the dector plane
is at the plane of least confusion. Comparison of 2a
to 2b shows that the compensating bend is better than
an on axis mirror.

PION   P =   6. HGMM   ZD =   −304.0580

ID=112 ENT 29442
SM=   .1920E+16
MN=   .1922
SD=   .3337E−01

INT. VS RADII AT DET. (CM)

II.E. Counter Design

The mechanical design of the counter had two major constraints, the desire to use the existing parabolic mirror and the physical layout of the NC2 enclosure. The mirror is 30cm in diameter and has a focal length of 3.05m. The NC2 enclosure is about 2.5m along the beamline by 3.6m transversely. [Figure II.E.1 shows a schematic of the counter].

The use of a plane mirror to extract the cerenkov light at 90 degrees in the horizontal plane allows the counter length in the enclosure to be 1m. The other 1.5m is then available for other beam monitoring devices. The 3m focal length then fits snuggly into the transverse dimension of the enclosure with the parabolic mirror and CCD on oppostive sides of the particle beam and behind the shielding of the berm.

The counter head is mechanically separated into two parts. The optical platform is a frame which holds the mirrors and the CCD rigidly together and connects them firmly to the ground and hence to the beam. The gas vessel encloses the frame and any motion it undergoes as the gas pressure is varied must be isolated from the frame. The vessel must hold one atmosphere on the outside and from 0 to 60Hgmm of helium gas on the inside.

II. E. 1   Schematic Layout of the Cerenkov Counter Head

Top View   Cerenkov Head
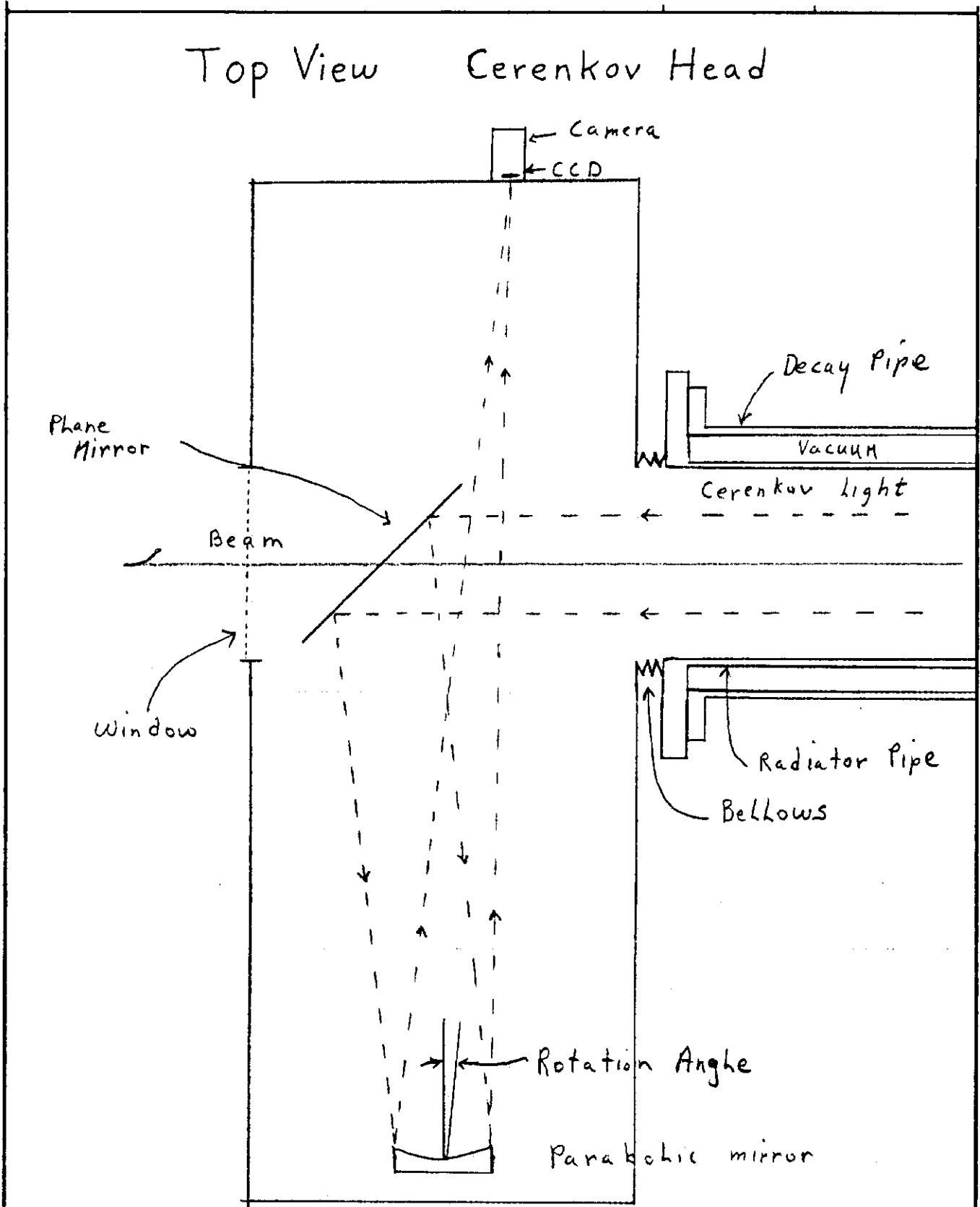
A 45cm diameter radiator pipe is connected to the counter head and penetrates upstream inside the 90cm diameter decay pipe. For safety reasons the radiator pipe must be rigid enough to withstand one atmosphere externally while at a vacuum internally. The pipe is designed in 2m sections with stiffening ribs and baffles at each end. The pipe sections are designed to be assembled and leak tested inside the enclosure as the entire assembly is pushed up into the decay pipe.

In conclusion it is seen that the necessity of using an off axis mirror to extract the light can be combined with the dual line source property of a beam line using a compensating bend technique to improve the cerenkov counter response. For the case studied with compensating bend it was shown that over 90% of the pion peak width is due to the beam spot sizes at the sources and over 90% of the kaon width is due to the beam momentum dispersion. It was also shown that a good π : k separation can be obtained at 500 GeV/c with a counter operating at low pressures and small angles.

I would like to thank Stephen Pordes for the many ways he helped in the design study and the preparation of this memo. I would also like to thank Dan Owen for his advice and Frank Taylor for his interest in and in checking important parts of the result.